J|A|C|S ARTICLES

Published on Web 08/16/2010

Atomic Structure of Au−Pd Bimetallic Alloyed Nanoparticles

Yong Ding,[†] Fengru Fan,[†,‡] Zhongqun Tian,[‡] and Zhong Lin Wang*[,†]

School of Materials Science and Engineering, Georgia Institute of Technology, Atlanta, Georgia 30332-0245, and Department of Chemistry, Xiamen University, Xiamen 361005, China

Received June 26, 2010; E-mail: zhong.wang@mse.gatech.edu

Abstract: Using a two-step seed-mediated growth method, we synthesized bimetallic nanoparticles (NPs) having a gold octahedron core and a palladium epitaxial shell with controlled Pd-shell thickness. The mismatch-release mechanism between the Au core and Pd shell of the NPs was systematically investigated by high-resolution transmission electron microscopy. In the NPs coated with a single atomic layer of Pd, the strain between the surface Pd layer and the Au core is released by Shockley partial dislocations (SPDs) accompanied by the formation of stacking faults. For NPs coated with more Pd (>2 nm), the stacking faults still exist, but no SPDs are found. This may be due to the diffusion of Au atoms into the Pd shell layers to eliminate the SPDs. At the same time, a long-range ordered $L1_1$ AuPd alloy phase has been identified in the interface area, supporting the assumption of the diffusion of Au into Pd to release the interface mismatch. With increasing numbers of Pd shell layers, the shape of the Au−Pd NP changes, step by step, from truncated-octahedral to cubic. After the bimetallic NPs were annealed at 523 K for 10 min, the SPDs at the surface of the NPs coated with a single atomic layer of Pd disappeared due to diffusion of the Au atoms into the surface layer, while the stacking faults and the $L1_1$ Au−Pd alloyed structure remained. When the annealing temperature was increased to 800 K, electron diffraction patterns and diffraction contrast images revealed that the NPs became a uniform Au−Pd alloy, and most of the stacking faults disappeared as a result of the annealing. Even so, some clues still support the existence of the $L1_1$ phase, which suggests that the $L1_1$ phase is a stable, long-range ordered structure in Au−Pd bimetallic NPs.

1. Introduction

Bimetallic nanoparticles (NPs) have received considerable attention recently for their unique optical, magnetic, and catalytic properties, which are very different from those of their monometallic NP components.[1] Among the bimetallic NPs, gold−palladium (Au−Pd) is one of the most attractive systems because of its promising use as a catalyst in CO oxidation, vinyl acetate monomer synthesis, hydrodechlorination of CCl_2F_2, hydrogenation of hydrocarbon, cyclotrimerization of acetylene, and so forth.[2−7] There are normally two approaches to synthesize Au−Pd bimetallic NPs: successive and simultaneous reduction of the metallic precursors.[8−11] The successive reduction approach normally gives better control of the shape and atomic ratio as compared to the simultaneous approach, and the synthesized Au−Pd bimetallic NPs show core−shell structure.

As we know, the chemical activity of these NPs is strongly determined not only by the particle size but also by the Au/Pd ratio at the surface.[12−15] Therefore, we need to characterize whether the Au and Pd components are chemically segregated or intimately alloyed in the synthesized NPs. According to the phase diagram, Au−Pd is likely to form solid solutions of arbitrary composition.[16] Further, the catalysts are normally used at high temperatures; thus, the structure stability and the species diffusion configuration are also important issues that need to be clarified.[2] Much research has been put into trying to figure out the atomic structure of Au−Pd core−shell NPs and their structural transformation upon annealing. Theoretically, both molecular dynamics simulation and density functional theory

[†] Georgia Institute of Technology.
[‡] Xiamen University.

(1) Burda, C.; Chen, X. B.; Narayanan, R.; El-Sayed, M. A. *Chem. Rev.* **2005**, *105*, 1025–1102.
(2) Chen, M. S.; Kumar, D.; Yi, C. W.; Goodman, D. W. *Science* **2005**, *310*, 291–293.
(3) Yi, C. W.; Luo, K.; Wei, T.; Goodman, D. W. *J. Phys. Chem. B* **2005**, *109*, 18535–18540.
(4) Wang, D.; Villa, A.; Porta, F.; Su, D. S.; Prati, L. *Chem. Commun.* **2006**, 1956–1958.
(5) Herzing, A. A.; Carley, A. F.; Edwards, J. K.; Hutchings, G. J.; Kiely, C. J. *Chem. Mater.* **2008**, *20*, 1492–1501.
(6) Heinz, H.; Farmer, B. L.; Pandey, R. B.; Slocik, J. M.; Patnaik, S. S.; Pachter, R.; Naik, R. R. *J. Am. Chem. Soc.* **2009**, *131*, 9704–9714.
(7) Naughton, J.; Lee, A. F.; Thompson, S.; Vinod, C. P.; Wilson, K. *Phys. Chem. Chem. Phys.* **2010**, *12*, 2670–2678.
(8) Fan, F. R.; Liu, D. Y.; Wu, Y. F.; Duan, S.; Xie, Z. X.; Jiang, Z. Y.; Tian, Z. Q. *J. Am. Chem. Soc.* **2008**, *130*, 6949–6951.
(9) Lee, Y. W.; Kim, M.; Kim, Z. H.; Han, S. W. *J. Am. Chem. Soc.* **2009**, *131*, 17036–17037.
(10) Lim, B.; Kobayashi, H.; Yu, T.; Wang, J. G.; Kim, M. J.; Li, Z. Y.; Rycenga, M.; Xia, Y. *J. Am. Chem. Soc.* **2010**, *132*, 2506–2507.
(11) Garcia-Gutierrez, D. I.; Gutierrez-Wing, C. E.; Giovanetti, L.; Ramallo-Lopez, J. M.; Requejo, F. G.; Jose-Yacaman, M. *J. Phys. Chem. B* **2005**, *109*, 3813–3821.
(12) Liu, H. B.; Pal, U.; Medina, A.; Maldonado, C.; Ascencio, J. A. *Phys. Rev. B* **2005**, *71*, 075403.
(13) Baddeley, C. J.; Barnes, C. J.; Wander, A.; Ormerod, R. M.; King, D. A.; Lambert, R. M. *Surf. Sci.* **1994**, *314*, 1–12.
(14) Atanasov, I.; Hou, M. *Surf. Sci.* **2009**, *603*, 2639–2651.
(15) Liu, F.; Wechsler, D.; Zhang, P. *Chem. Phys. Lett.* **2008**, *461*, 254–259.
(16) Okamoto, H.; Massalski, T. B. *Bull. Alloy Phase Diagrams* **1985**, *6*, 7.

10.1021/ja105614q

predict that the stable ordered structures of the bimetallic NPs have a Pd core and a Au shell.[12,17−19] Although NPs having a Au core and a Pd shell can be formed at low temperatures, with increasing temperature the Au atoms prefer to migrate to the outer shell. *Ab initio* calculations on the stability of Au−Pd alloy phases suggest that a multitude of ground states exist, especially at the Au-rich side. Possible long-range order phases occur near the composition $Au_{70}Pd_{30}$.[20,21] Experimentally, using transmission electron microscopy (TEM) and scanning transmission electron microscopy (STEM), a three-layer core−shell structure in Au−Pd bimetallic NPs has been identified,[22,23] revealing an evenly alloyed inner core, a Au-rich intermediate layer, and a Pd-rich outer shell. The Au−Pd alloy phases have been observed after heat treatment at 773 K.[24−26] Long-range ordered structures with {001}-type ordering have been reported in Au−Pd thin films. They are $L1_2$-type around compositions Au_3Pd, L1-type around $AuPd_3$, and $L1_0$-type around AuPd.[27−29] However, no ordered phase has been reported in Au−Pd bimetallic NPs.

Considering the different atomic radii of Au and Pd, strain is built up at the core−shell interface, although it is small, around 4.6%.[30,31] But if the strain can be released by the formation of defects or by dislocation (for example, misfit dislocations), then the system energy may be dramatically reduced. Although much effort has gone into structure determination from both theoretical calculations and experimental observations, as listed above, there have been no reports of an interface strain release configuration in the system. In this work, by using high-resolution transmission electron microscopy (HRTEM), we have systematically investigated the interface structure of Au−Pd core−shell NPs. Single-crystal Au octahedra of size ∼11 nm were chosen as the cores. The thickness of the Pd epitaxial shell was tailored from one atomic layer to ∼2 nm thick and later to ∼5 nm thick to trace the mismatch-release mechanism. The Au−Pd bimetallic NPs were also annealed at high temperatures to investigate the stability of the structures.

2. Experimental Section

Au NPs of about 11 nm in diameter were first synthesized by a modified seed-mediated growth method.[32] A 10 mL aqueous solution containing $HAuCl_4$ (0.25 mM) and cetyl trimethylammonium bromide (CTAB, 75 mM) was prepared in a flask. Into this mixture, 0.6 mL of ice-cold $NaBH_4$ (10 mM) was rapidly injected with vigorous stirring, generating a brown solution. The solution was stirring slowly in a water bath at 308 K for 3 h. For the seed solution, 4 mL of prepared hydrosol was diluted to 100 mL with water. A colorless mixture of 0.1 mL of $HAuCl_4$ (10 mM), 2 mL of CTAB (0.2 M), and 1.5 mL of ascorbic acid (AA, 0.1 M) was diluted to 25 mL, and then 2 mL of seed hydrosol was added immediately. The reaction mixture was shaken and then left undisturbed in the same water bath for 8 h. Finally, a typical pale purple colloid was observed, indicating the formation of Au NPs. The preparation of Au−Pd core−shell NPs was similar to that reported previously.[8] By adjusting the volume of added H_2PdCl_4 solution, we successfully controlled the thickness of the Pd shell: to control the Pd shell from one atomic layer to several layers, and finally to form the nanocubes, 20 μL, 100 μL, and 0.5 mL portions of H_2PdCl_4 solution were added to the prepared Au NPs solution. The mixture was shaken and then left undisturbed in a water bath at 308 K for about 6 h, and the color of the hydrosol changed from pale purple to brown.

The synthesized NPs were centrifuged (12 000 rpm, 30 min) and then washed twice with water. The precipitate was collected, redispersed in water, and then dropped onto Ni grids for TEM study. A JEOL 4000EX instrument was used to record the HRTEM images, operated at 400 keV. A FEI G2 F20 transmission electron microscope working in STEM mode was used to record the high-angle annular dark-field (HAADF) images of the bimetallic NPs. The *in situ* heating experiments were monitored by using a Hitachi HF2000 transmission electron microscope working at 200 keV. Cerius 2 and MacTempas softwares were used for HRTEM simulation.

3. Results and Discussion

Figure 1a−c gives low-magnification TEM bright-field and dark-field images and the diffraction pattern of Au octahedral seeds. The average size of these particles is ∼11 nm. After one atomic layer of Pd was coated onto the Au octahedral core, there were no observable changes in the low-magnification TEM images and the diffraction pattern (Figure 1d−f). When more Pd (layer around 2 nm thick) was coated onto the Au core, the strain induced by the mismatch between Au core and "Pd shell" (later we will show that it is actually a Au−Pd alloy shell instead of a pure Pd shell) was revealed by the diffraction contrast images (Figure 1g,h). The diffraction pattern actually contains two sets of rings coming from the Au cores and Pd shells, respectively. The inset of Figure 1i shows two separate {220} diffraction rings from the core and shell, respectively.

The HRTEM images of a Au octahedral seed and a core−shell NP coated with one atomic layer of Pd are displayed in Figure 2a,b. The incident electron beam direction is along [110]. The side surfaces of the particles can be indexed as {111} and {100} planes, as labeled in Figure 2. Actually, the real shape of these particles is truncated-octahedron. The Pd-coated NP has some defects at the {111} surface. In order to see the defects clearly, Figure 2c gives a magnification of the rectangle-enclosed area in Figure 2b. We know that the standard stacking sequence of close-packed {111} planes is ABCABC... in face-centered cubic (FCC) structures; however, after one layer of Pd atoms was coated on the Au seed, this sequence was no longer

(17) Boscoboinik, J. A.; Plaisance, C.; Neurock, M.; Tysoe, W. T. *Phys. Rev. B* **2008**, *77*, 045422.
(18) Yuan, D. W.; Gong, X. G.; Wu, R. Q. *Phys. Rev. B* **2008**, *78*, 035441.
(19) Liu, H. B.; Pal, U.; Perez, R.; Ascencio, J. A. *J. Phys. Chem. B* **2006**, *110*, 5191–5195.
(20) Sluiter, M. H. F.; Colinet, C.; Pasturel, A. *Phys. Rev. B* **2006**, *73*, 174204.
(21) Barabash, S. V.; Blum, V.; Muller, S.; Zunger, A. *Phys. Rev. B* **2006**, *74*, 035108.
(22) Ferrer, D.; Torres-Castro, A.; Gao, X.; Sepulveda-Guzman, S.; Ortiz-Mendez, U.; Jose-Yacaman, M. *Nano Lett.* **2007**, *7*, 1701–1705.
(23) Ferrer, D.; Blom, D. A.; Allard, L. F.; Mejia, S.; Perez-Tijerina, E.; Jose-Yacaman, M. *J. Mater. Chem.* **2008**, *18*, 2442–2446.
(24) Jana, D.; Dandapat, A.; De, G. *J. Phys. Chem. C* **2009**, *113*, 9101–9107.
(25) Perez-Tijerina, E.; Mejia-Rosales, S.; Inada, H.; Jose-Yacaman, M. *J. Phys. Chem. C* **2010**, *114*, 6999–7003.
(26) Mejia-Rosales, S. J.; Fernandez-Navarro, C.; Perez-Tijerina, E.; Montejano-Carrizales, J. M.; Jose-Yacaman, M. *J. Phys. Chem. B* **2006**, *110*, 12884–12889.
(27) Nagasawa, A.; Matsuo, Y.; Kakinoki, J. *J. Phys. Soc. Jpn.* **1965**, *20*, 1881.
(28) Matsuo, Y.; Nagasawa, A.; Kakinoki, J. *J. Phys. Soc. Jpn.* **1966**, *21*, 2633.
(29) Nagasawa, A. *J. Phys. Soc. Jpn.* **1964**, *19*, 2344.
(30) International Centre for Diffraction Data. *The Powder Diffraction File*; ICDD: Newtown Square, PA, 2010; ICDD PDF00-005-0681.
(31) International Centre for Diffraction Data. *The Powder Diffraction File*; ICDD: Newtown Square, PA, 2010; ICDD PDF00-004-0784.
(32) Sau, T. K.; Murphy, C. J. *J. Am. Chem. Soc.* **2004**, *126*, 8648–8649.

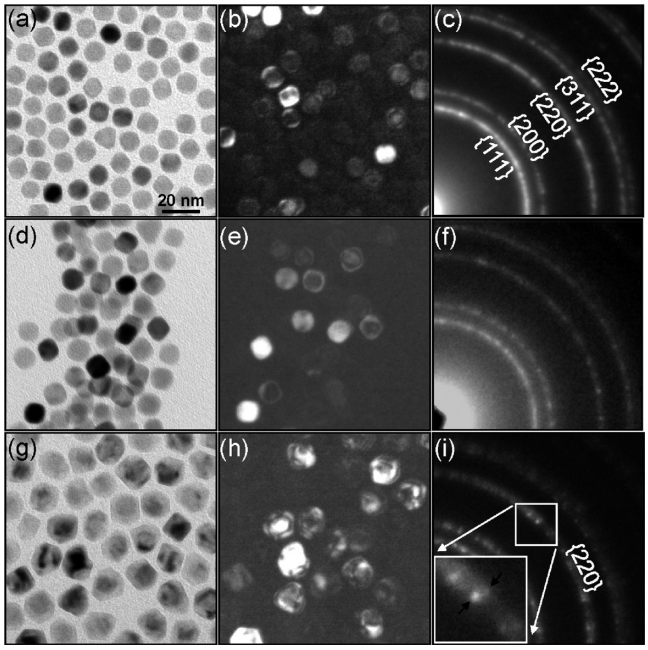

Figure 1. Low-magnification bright-field (left) and dark-field (middle) TEM images and their corresponding diffraction patterns (right) for Au seeds (a−c) and one layer Pd-coated (d−f) and ∼2 nm Pd-coated (g−i) bimetallic nanoparticles.

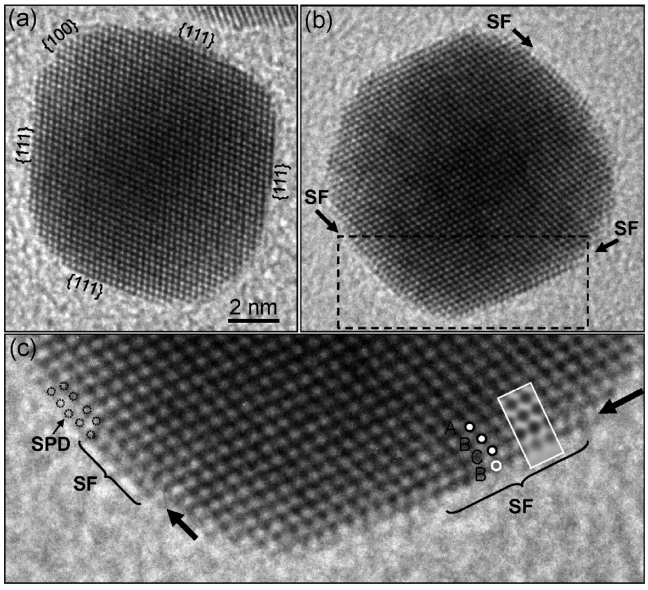

Figure 2. HRTEM images of (a) a Au seed and (b) a bimetallic nanoparticle coated with a single atomic layer of Pd. (c) Magnified HRTEM image from the rectangle-enclosed area in (b).

followed. Instead, the sequence became ABCB, as shown in Figure 2c. Because such a stacking-sequenced structure is missing one layer compared to the standard FCC structure, we named it as a stacking fault (SF) structure. An atomic model of the SF structure is displayed in Figure 3a, with the Pd in the first surface layer. On the basis of the atomic model, HRTEM simulation was carried out. The best matching result is shown in Figure 2c, with a sample thickness of 3.9 nm.

The formation of stacking faults in Au−Pd core−shell structure can be linked to Shockley partial dislocations (SPDs).[33] Because of the different lattice parameters between Au and Pd (4.079 and 3.8898 Å, respectively), there is ∼4.6% mismatch

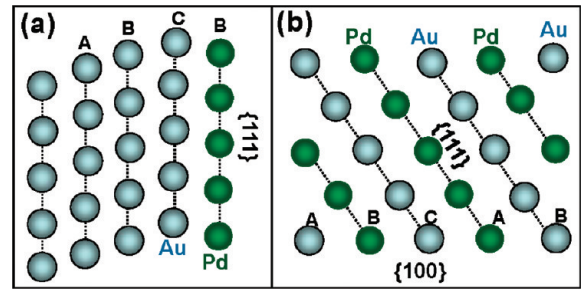

Figure 3. Atomic models of (a) a stacking fault structure and (b) an $L1_1$ AuPd alloy structure.

between the Au core and Pd shell. The formation of mismatch dislocations is a proper way to release the mismatch. Considering that the interfaces are dominated by {111} planes and the Burgers vector of a SPD in FCC structure is $a/6\langle 112\rangle$ (a is the lattice parameter), which lies inside the {111} planes, the SPDs can serve as the mismatch dislocations in our Au−Pd interface to release the strain caused by mismatch. We do observe them in the HRTEM image. The arrow in Figure 2c highlights one of the SPDs. However, a partial dislocation cannot exist independently; it has to combine with a stacking fault. That is why we see stacking faults in NPs coated with one atomic layer of Pd. Therefore, the formation of stacking faults is indirectly linked to the mismatch release, and further, the stacking fault marks the location of the Au-core/Pd-shell interface.

It is difficult to separate Pd atoms from Au ones solely on the basis of their contrast in HRTEM images. Such SPD-combined SF structure gives us a useful clue to track the coated Pd. For a pure Au octahedron, there have been no reports on stacking faults in the surface layer, to the best of our knowledge. We have identified three stacking faults from the {111} side surfaces of the Au−Pd NP in Figure 2b, indicated by black arrows. The top-left {111} surface is free from stacking faults. This suggests that the Pd coating was not uniform.

In order to understand how the Pd shells build up, we coated more Pd (∼2 nm thick on average) onto the Au seeds, but still keeping the truncated-octahedron shape. The low-magnification TEM images are displayed in Figure 1g. A HRTEM image from one of the core−shell Au−Pd NPs is displayed in Figure 4a. The center dark-contrast area enclosed by dashed lines corresponds to the Au octahedron core. The Pd shell shows light contrast due to the weaker scattering power of Pd atoms compared to that of Au. Four stacking faults can be identified in the HRTEM image, as indicated by black arrows. One of them is located at the core−shell interface area, but the others are close to the shell surface. A magnified image of the bottom-right stacking fault is shown separately in Figure 4b. Among these four stacking faults, only one end of one stacking fault (totally eight ends) terminated inside the particles. Therefore, only one partial dislocation can be confirmed. There were no other SPDs accompanying the stacking fault. Considering the lattice parameters of FCC Au and Pd, ideally, the stacking fault cannot be longer than 5.5 nm (see Supporting Information, S1)—any longer and the mismatch between the {111} planes of Au and Pd will make the system unstable. A possible reason is that a large Au atom diffused from the inside core to the surface Pd layer and eliminated the SPD. Besides the stacking

(33) Singh, S. R.; Howe, J. M. *Philos. Mag. A* **1992**, *66*, 739–771. See also: http://www.tf.uni-kiel.de/matwis/amat/def_en/kap_5/backbone/r5_4_1.html.

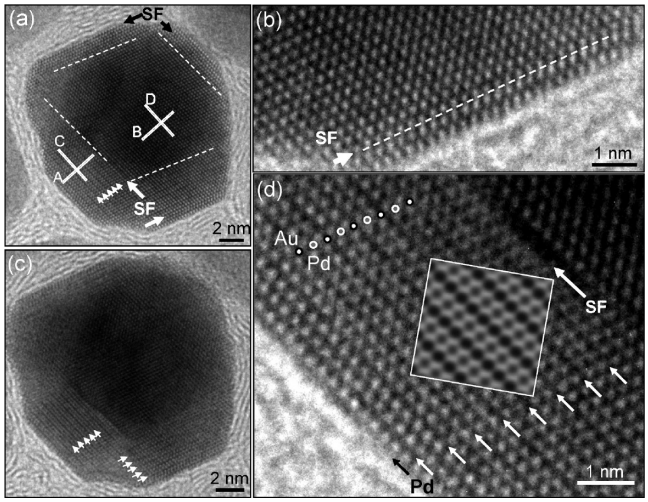

Figure 4. (a,c) HRTEM images of the same ~2 nm Pd-coated Au−Pd nanoparticle recorded at different focus conditions. (b) Magnified HRTEM image showing the stacking fault in the bottom-right area of (a). (d) Magnified HRTEM image from the bottom-left part of (a); inset is a simulated HRTEM image based on the structure model illustrated in Figure 3b.

faults, a long-range order structure in the bottom-left part of the shell can be identified. After refocusing the transmission electron microscope, such long-range ordering can be seen much more clearly in Figure 4c. At the same time, such long-range ordering also exists in the bottom-right area, indicated by white arrows. An enlarged HRTEM image from the bottom-left part of the NP is shown in Figure 4d. Considering that only Au and Pd exist in the NPs (X-ray energy-dispersive spectra (EDS) results not shown here), there are two possibile explanations for such periodic variation of the contrast in the {111} planes. First, it may be due to the ordered vacancies. However, in order to cause such a contrast difference, the density of the vacancies in one close-packed {111} plane would be too high, making the structure unstable. Second, it may be due to the formation of long-range ordered Au−Pd alloy structure as a result of diffusion of some Au atoms from the core into the shell layer. In the phase diagram of the Au−Pd system, the reported long-range ordered structures include $L1_2$ (Au_3Pd), $L1_0$ (AuPd), and L1 ($AuPd_3$).[27−29] However, none of them has the ordering along the ⟨111⟩ direction as shown in Figure 4. Instead, such a structure can be categorized as an $L1_1$ alloy structure. The $L1_1$ long-range ordered phase is popular in CuPt alloy systems,[34−36] and the structural model is illustrated in Figure 3b. In contrast to the disordered FCC alloy structure, what makes the ordering of $L1_1$ unique is that the alloy atoms normal to the ⟨111⟩ direction are arranged in alternating layers of pure Cu and pure Pt (here in our system is pure Au and pure Pd). In this ordered structure, the ideal atomic ratio between Au and Pd is 1:1. The simulated HRTEM image based on the structure model as illustrated in Figure 3b is inset in Figure 4d. It matches the experimental one fairly well. Simulated images with different thicknesses and defocus conditions can be found in the Supporting Information (S2). The corresponding Au and Pd layers have been indexed as well. In this situation, the first surface layer of the shell can be identified as Pd, or at least Pd-rich. Because of the diffusion of Au atoms from the core to the shell, it is not simply a Au−Pd core−shell structure anymore. It is more appropriate to refer to it as a Au−AuPd core−shell structure.

Both the absence of SPDs and the existence of the long-range ordered $L1_1$ AuPd alloy phase in the NPs supports the diffusion of Au atoms from the core into the shell. Although Au has a lower surface energy than that of Pd (1.63 and 2.05 J/m^2, respectively),[37,38] Au is expected to preferentially segregate to the surface. But the Au-core/Pd-shell structure changes to Pd-core/Au-shell after annealing at about 773 K, as predicted by the molecular dynamics simulation.[12] Our whole synthesis process was kept at 308 K. Therefore, the diffusion of Au in the Au−Pd bimetallic NPs is not solely based on the requirement of minimization of surface energy. There must be another mechanism that drives the Au atoms to diffuse out of the core. It is possible that the interface mismatch strain might drive the gradient distribution of Au atoms from the core to the surface. Considering the lattice parameters of pure Au and Pd, the formation of an alloy phase can release the lattice mismatch between the core and shell (the lattice parameter of Au:Pd = 1:1 alloy is 0.39843 Å according to the phase diagram, which is in between the lattice parameters of pure Au and pure Pd).[16] We measured the difference in the planar distance between the core and shell areas by line profiles, as shown in Figure 5. The line profiles from lines A and B in Figure 4a along the direction normal to the {111} plane are shown in Figure 5a,b. The line profiles from lines C and D inside the {111} planes are shown in Figure 5c,d. The long-range ordering in the [111] direction, emphasized by arrows, can be seen clearly in the line profile image in Figure 5a. The planar distance of the {111} plane in the ordered area is 98.5% of that in the Au core, while inside each {111} plane, the distance between nearby atoms from the alloy areas is just 96.2% of that in the Au core area, as measured from the profiles in Figure 5c,d. The different ratios inside and normal to the {111} plane between alloy and pure Au provide further evidence of the formation of $L1_1$ alloy structure. Because of the unequal atomic radii of Au and Pd, the ordered structure is no longer a FCC structure, but shows rhombohedral distortion.[39] If the shell were composed purely of Pd atoms, then the lattice parameter ratio between core and shell will be 1:0.956.[16] The formation of $L1_1$ alloy phase at the core−shell interface definitely reduced the mismatch. In other words, the stress building up at the core−shell interface drives the diffusion of Au atoms out from the core. Therefore, in our Au−Pd NP system, the interface mismatch is released by the diffusion of Au atoms. The formation of $L1_1$ alloy phase is a strong evidence to support the Au diffusion scenario.

As we know from Figure 2b, the first coated Pd layer will form stacking faults at the {111} surfaces, for they are introduced by the SPDs, which release the interface mismatch energy. Therefore the position of the stacking faults mark the location of the core−shell interface. However, as shown in Figure 4, only one stacking fault locates at the assumed core−shell interface, while the other three are close to the shell surface. The location of the assumed core−shell interface is based on the contrast difference and the known real size of the octahedral seeds. This inconsistency also supports the diffusion of Au atoms out from the core.

(34) Sun, A. C.; Yuan, F. T.; Hsu, J. H.; Lee, H. Y. *Scr. Mater.* **2009**, *61*, 713–716.
(35) Lang, H.; Mohri, T.; Pfeiler, W. *Intermetallics* **1999**, *7*, 1373–1381.
(36) Iwata, S.; Yamashita, S.; Tsunashima, S. *IEEE Trans. Magn.* **1997**, *33*, 3670–3672.
(37) Mezey, L. Z.; Giber, J. *Surf. Sci.* **1982**, *117*, 220–231.
(38) Tyson, W. R.; Miller, W. A. *Surf. Sci.* **1977**, *62*, 267–276.
(39) Johansson, C. H.; Linde, J. O. *Ann. Phys.-Berlin* **1927**, *82*, 449–478.

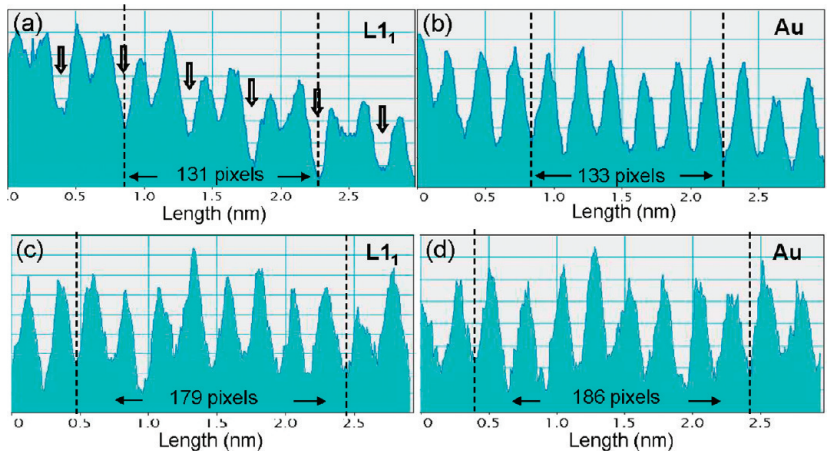

Figure 5. Line profile images from the lines (a) **A**, (b) **B**, (c) **C**, and (d) **D** in Figure 4a.

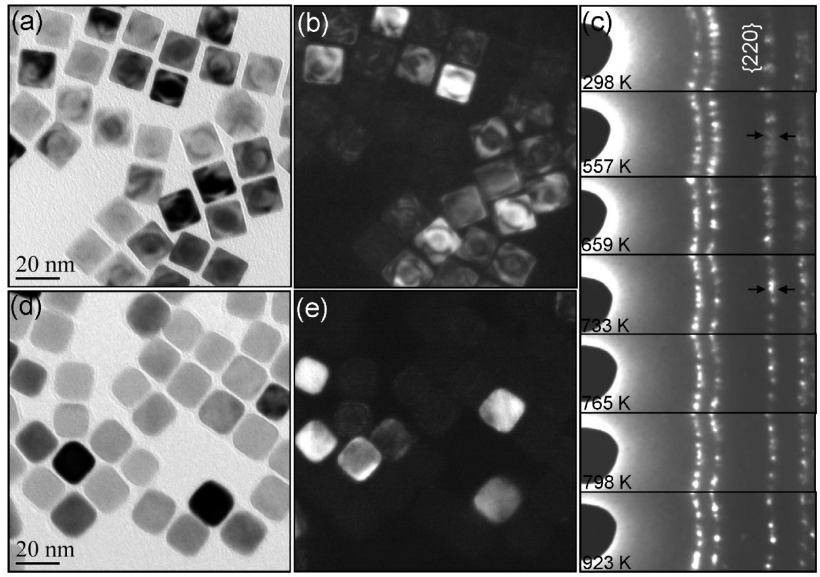

Figure 6. (a,d) Bright-field and (b,e) dark-field TEM images of Au−Pd nanocubes before (top) and after (bottom) annealing. (c) Diffraction patterns recorded at different temperatures.

As more and more Pd is coated on the Au seeds, finally the shape of the bimetallic NPs turns to nanocube, as shown in Figure 6a,b. The strain field located at the core−shell interface can be seen clearly. A HRTEM image from a single Au−Pd nanocube is displayed in Figure 7a, with an incident electron beam along the [001] direction. If the reported long-range ordered structures $L1_2$ (Au_3Pd), $L1_0$ (AuPd), and L1 ($AuPd_3$) do exist in our Au−Pd bimetallic NPs, then we can identify their long-range ordering in the ⟨100⟩ direction from the HRTEM image shown in Figure 7a. However, we do not observe such ordering in the image. Instead, a ×2 reconstruction in the {100} surfaces is identified in Figure 7a, and its magnified image is displayed in Figure 7b. The core−shell structure is clearly indicated by the different contrast in the HAADF image displayed in Figure 7c.

In order to investigate the thermal stability of the Au−Pd bimetallic NPs, *in situ* heating experiments were carried out in a TEM high-vacuum chamber. The temperature-dependent diffraction patterns from the nanocubes are displayed in Figure 6c. The formation of a uniform alloy phase can be tracked through the changes of the diffraction rings. Taking the {220} diffraction ring as an example, it contains two separate rings coming from the core and shell at room temperature; the two rings merge into one as the temperature reaches 733 K, above which there is no change in the diffraction patterns. The core−shell interface disappears and the nanocubes show uniform contrast in the bright-field (Figure 6d) and dark-field (Figure

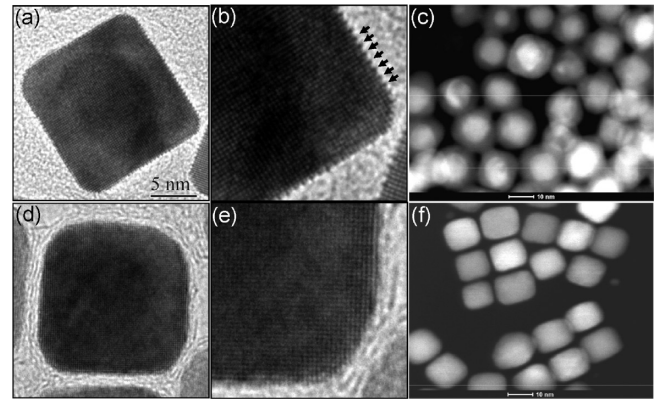

Figure 7. HRTEM images from the Au−Pd nanocube before (a,d) and after (b,e) annealing, and HAADF images from the Au−Pd nanocubes before (c) and after (f) annealing.

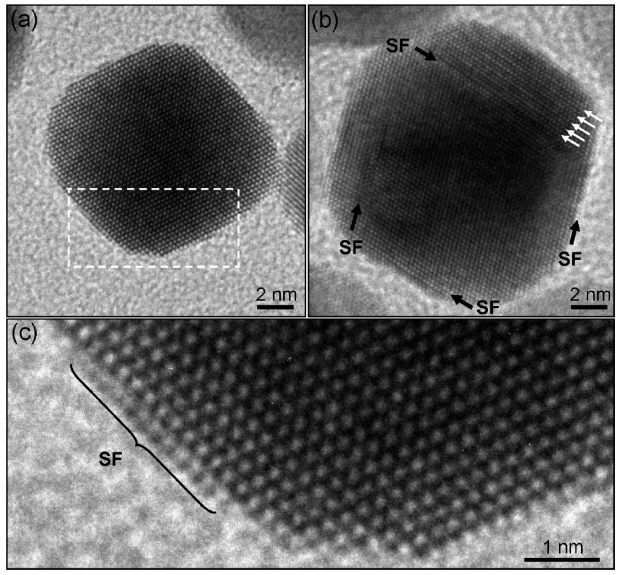

Figure 8. (a,b) HRTEM images of bimetallic nanoparticles coated with one atomic layer and ~2 nm of Pd after annealing at 523 K for 10 min. (c) Magnified HRTEM from the area enclosed by the rectangle in (a).

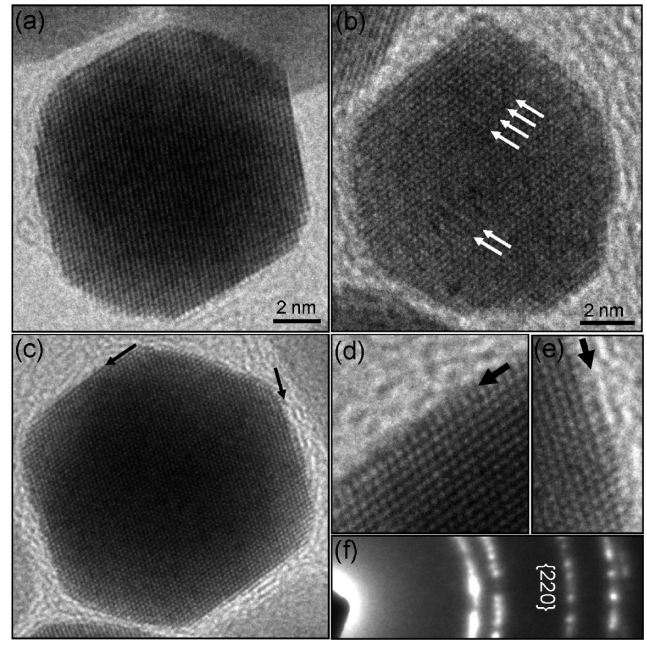

Figure 9. (a,b) HRTEM images from bimetallic nanoparticles coated with one atomic layer of Pd after annealing at 800 K for 10 min. (c−f) HRTEM images and diffraction pattern from bimetallic nanoparticles coated with ~2 nm Pd after annealing at 800 K.

6e) TEM images. The HRTEM image from one of the annealed nanocubes is shown in Figure 7d. A magnified image from the bottom-right corner of the nanocube is shown in Figure 7e. There is no long-range ordering; just the FCC structure image projected along [001] direction is seen. The HAADF image in Figure 7f indicates uniform contrast of the nanocubes, suggesting the homogenizing distribution of Au and Pd.

Annealing experiments were also carried out on the bimetallic NPs coated with one atomic layer and ~2 nm Pd. As we know that typical reactions using Au−Pd catalysts are normally carried out below 500 K,[2] we first annealed the NPs at 523 K for 10 min. Based on the *in situ* results shown in Figure 6c, we know that the core−shell structure still survives at this temperature. The HRTEM images of the NPs after annealing are displayed in Figure 8. For the NP coated with a single atomic layer of Pd, shown in Figure 8a, a stacking fault at the bottom-left {111} surface can be identified, as shown in the magnified image in Figure 8c, but no SPD accompanies it. It must be due to diffusion of Au atoms into the surface layer. For ~2 nm Pd-coated NP shown in Figure 8b, the $L1_1$ long-range ordering area is emphasized by a group of white arrows. The four stacking faults parallel to the four {111} surface planes are marked by black arrows. Again, no SPDs are found in the vicinity of the stacking faults. The results shown in Figure 8 indicate that more Au atoms diffused out and the $L1_1$ long-range ordered structures are stable after annealing at 523 K.

After further annealing at 800 K for 10 min, there is no longer a clear core−shell interface. The HRTEM images recorded for the two samples are shown in Figure 9. For the NPs coated with one atomic layer of Pd, there is no stacking fault at the surface of the truncated-octahedron, as shown in Figure 9a. In another NP, shown in Figure 9b, white arrows mark the local $L1_1$ long-range ordering, although the contrast is weak. This means that most of the Pd atoms at the surface layer diffused inside of the NP after annealing at such a high temperature. Figure 9c gives the HRTEM image of a NP coated with ~2 nm Pd after annealing. In contrast to the HRTEM images recorded before annealing, there is no defect inside the NP. The long-range ordered $L1_1$ structure is not observed. However, two stacking faults at the first surface layer can be identified, which are shown separately in Figure 9d,e. Because no SPDs are seen in combination with the stacking faults, the surface layer cannot be pure Pd. It must be a Au−Pd mixed layer, although we cannot precisely identify the species of each atoms on the basis of the techniques we used. The diffraction pattern shown in Figure 9f indicates that there is only one set of diffraction ring patterns, compared with that shown in Figure 1i. This means a uniform alloy phase has formed.

4. Conclusion

Using high-resolution transmission electron microscopy, we systematically studied the interface mismatch-release mechanism of Au−Pd bimetallic nanoparticles and the thermal stability of the nanoparticles. The major results can be summarized as follows:

1. When only a single atomic layer of Pd is coated onto the Au core, the mismatch strain is released by the formation of Shockley partial dislocations, which are accompanied by stacking faults. The existence of such stacking faults can be considered as a criterion to identify whether the Pd is coated on the Au core.

2. When more Pd is coated on the Au core, the mismatch-release is dominated by Au diffusion from the core to the shell. The disappearance of Shockley partial dislocations and the formation of the long-range ordered $L1_1$ Au−Pd alloy structure support the assumption of Au diffusion.

3. After annealing at 523 K, more Au diffuses out. The Shockley partial dislocations in the nanoparticles coated with one atomic layer of Pd disappeared as well. While the $L1_1$ alloy phase is stable at such temperature, the core−shell structure will be destroyed, and a uniform alloy structure will form after annealing at 800 K.

4. The $L1_1$ alloy phase with Au:Pd = 1:1 is the only long-range ordered structure confirmed by our TEM study.

Acknowledgment. The authors thank Dr. LinFen Fu and Y. C. Wang from FEI Company for their help in STEM work. This research was supported by BES DOE (DE-FG02-07ER46394), NSF (DMS0706436, CMMI 0403671), KAUST Global Research Partnership, National Institute for Materials, Japan (Agreement DTD 1 Jul 2008), Samsung, and Korea Electronic Technology Institute (KETI).

Supporting Information Available: Atomic model showing mismatch between Au and Pd; simulated HRTEM images of $L1_1$ phase at different thicknesses and defocus conditions. This material is available free of charge via the Internet at http://pubs.acs.org.

JA105614Q